European Journal of Medicinal Chemistry 180 (2019) 340–349

Contents lists available at ScienceDirect

European Journal of Medicinal Chemistry

journal homepage: http://www.elsevier.com/locate/ejmech

Research paper

# Variations on a scaffold - Novel $GABA_A$ receptor modulators

Maria Teresa Iorio [a], Sabah Rehman [b], Konstantina Bampali [b], Berthold Stoeger [a], Michael Schnürch [a], Margot Ernst [b], Marko D. Mihovilovic [a, *]

[a] TU Wien, Institute of Applied Synthetic Chemistry, Getreidemarkt 9/163-OC, 1060, Vienna, Austria
[b] Medical University of Vienna, Center for Brain Research, Spitalgasse 4, 1090, Vienna, Austria

ARTICLE INFO

*Article history:*
Received 10 April 2019
Received in revised form
2 July 2019
Accepted 2 July 2019
Available online 5 July 2019

*Keywords:*
$GABA_A$ receptors
Pyrazoloquinolinones
Allosteric modulators
Pharmacophore

ABSTRACT

Allosteric ligands of $GABA_A$ receptors exist in many different chemotypes owing to their great usefulness as therapeutics, with benzodiazepines being among the best known examples. Many allosteric binding sites have been described, among them a site at the extracellular interface between the alpha principal face and the beta complementary face (α+/β-). Pyrazoloquinolinones have been shown to bind at α+/β- binding sites of $GABA_A$ receptors, exerting chiefly positive allosteric modulation at this location. In order to further explore molecular determinants of this type of allosteric modulation, we synthesized a library of ligands based on the PQ pharmacophore employing a ring-chain bioisosteric approach. In this study we analyzed the structure-activity-relationship (SAR) of these novel ligands based on an azo-biaryl structural motif in α1β3 $GABA_A$ receptors, indicating interesting novel properties of the compound class.


## 1. Introduction

$GABA_A$ receptors are pentameric ligand-gated ion channels and belong to the cys-loop receptor superfamily. They are arranged in homo- or heteropentameres, which are assembled from a pool of 19 different subunits producing a large variety of receptor subtypes with distinct pharmacology. The most common receptor is formed by 2α, 2β and 1γ subunits. In the binary receptors, the γ subunit that forms the interface where the BDZ binding site is placed (α+/γ-), is thought to be replaced by an additional β subunit [1]. The five subunits forming the pentamer are arranged in counter clockwise fashion e.g. αβαββ, forming five±interfaces (α+/β-; β+/α-; α+β-; β+/β-; β+/α with GABA sites being formed by the β+/α-interfaces) in the case of binary αβ receptors (Fig. 1, panel A).

$GABA_A$ receptors contain a relatively large number of allosteric binding sites and, consequently, also a large and chemically diverse set of allosteric ligands of $GABA_A$ receptors exist. Among the allosteric modulators, pyrazoloquinolinones (PQs) (Fig. 1, panel B) have been largely investigated for their pharmacological properties starting from the 1980s [2]. They were predominantly described as high affinity ligands binding at the benzodiazepine binding site (historically termed benzodiazepine-receptors) [3]. More recent functional studies revealed that PQs modulate $GABA_A$ receptors by interacting with an alternative site at the extracellular interface between the alpha principal face and the beta complementary face (α+/β-). Given the existence of six alpha and three beta isoforms, in theory eighteen such sites may be present and potentially suitable to target distinctive receptor isoforms [4–6]. Thus, many modifications of the general PQ scaffold were generated for identifying subtype-selective compounds [6,7].

Here we aimed to generate a novel scaffold that is strongly inspired by the pharmacophoric descriptors of pyrazoloquinolinones that may lend itself to substantial improvements both in terms of pharmacokinetic and ADMET properties as well as the potential for subtype selectivity. Even though many chemotypes have been described already targeting this family of receptors, many challenges remained unmet [8]. This is in part due to the high homology among subunits, which makes it difficult to develop and to characterize genuinely selective substances as many of the interaction sites for allosteric modulators contain highly conserved ligand recognition motifs [9]. Interestingly, so far only few of the existing interaction sites for allosteric modulators have been targeted extensively by compound development efforts. Traditionally, ligands for the benzodiazepine recognition sites have

*Abbreviations:* GABA, gammaaminobutirric acid; PQ, pyrazoloquinolinones.

* Corresponding author.
*E-mail addresses:* maria.iorio@tuwien.ac.at (M.T. Iorio), sabah.rehman@meduniwien.ac.at (S. Rehman), konstantina.bampali@outlook.com (K. Bampali), berthold.stoeger@tuwien.ac.at (B. Stoeger), michael.schnuerch@tuwien.ac.at (M. Schnürch), margot.ernst@meduniwien.ac.at (M. Ernst), marko.mihovilovic@tuwien.ac.at (M.D. Mihovilovic).

https://doi.org/10.1016/j.ejmech.2019.07.008

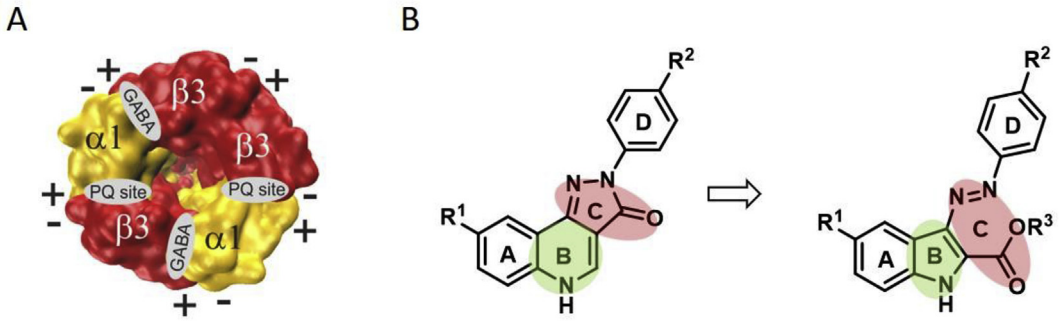


**Fig. 1.** Panel A top view of α1β3 $GABA_A$ receptor; Panel B PQ general structure and proposed modifications of the scaffold of PQ: reduction of the size of ring B (green) and opening of ring C (red). (For interpretation of the references to colour in this figure legend, the reader is referred to the Web version of this article.)

been developed towards subtype selectivity [8,10].

Considerable efforts were directed also towards ligands that target so-called anesthetic sites, which are a heterogenous group of binding sites that are localized in the transmembrane domain [9,11]. The allosteric sites that are present in the extracellular domain, such as the high affinity benzodiazepine site at the extracellular α+/γ− interfaces and the modulatory PQ site at the α+/β− interfaces display much higher variability in sequence and local structure, compared to the highly conserved transmembrane domain, and are thus considered superior candidates for the development of selective compounds [5].

In this work we describe the design, synthesis and biological properties of a series of new compounds with a highly similar pharmacophore as displayed by the PQs in α1β3 $GABA_A$ receptors, for which the most extensive exploration of differently substituted pyrazoloquinolinone's modulatory properties is available [12]. While this receptor subtype is of relatively low abundance in the mammalian brain [4,13], it has numerous advantages for the expression in heterologous cell systems and for the pharmacological testing of compounds that only require alpha and beta subunits for their activity [12,14]. For the purposes of this study, this receptor composition offers the advantage of lacking the benzodiazepine binding site and thus reducing the number of potentially interfering additional allosteric effects.

## 2. Results and discussion

### 2.1. Pharmacophore features and ligand-design

The most common modifications of the pyrazoloquinolinones scaffold concern ring A and ring D, which were modified both in terms of position of substituents and dimension of the ring. For example, as reported by Varagic et al. [12], changes in the position of the substituents on ring A had significant impact on the potency of the PQ derivatives, whereas in combination with changes in the position and functional group of the substituent on ring D influenced the modulatory efficacy of different receptor subtypes [12]. In the same work, the replacement of ring A with an aliphatic ring resulted in a null modulator at the benzodiazepine (BZ) binding site, and the replacement with a thiophene led to the synthesis of a non-binder. Modifications on rings B and C are less investigated: the replacement of the pyrazolo ring C with a triazolo system gave compounds with high affinity for the α+/β-binding site [15]. In order to gain more insight on the effect of changes of ring B and C, we designed a new scaffold with several modifications (Fig. 1, panel B).

More specifically the pyridine ring is replaced by a pyrrole moiety, leading to a reduction in the size of ring B; and the pyrazolone which formed ring C is opened following the concept of ring-chain bioisosterism. Moreover, a carboxylic acid group is attached to ring B and the D ring is connected to the core of the molecule via an azo group. The insertion of a carboxylic acid function was considered in order to increase the poor solubility, which would help to overcome one of the major issues of the pyrazoloquinolinones [16]. Before starting the actual synthesis, the pharmacophores of PQs and of the new scaffold were generated and compared with the program LigandScout 4.2.1 available from Inte:Ligand GmbH [17,18], in order to assess whether the new compound class could potentially occupy the same binding site. As shown in Fig. 2a, the pharmacophore of PQ consists of eight features: two hydrophobic features - ring A and D -, two hydrogen bond acceptors - the nitrogen and the ketone of the pyrazolo ring -, depicted as yellow and red spheres respectively; three aromatic rings - labelled A, B and D -, and one hydrogen bond donor — quinoline nitrogen-represented with blue rings and a green arrow respectively. In the indole-derivative pharmacophore, all these features are conserved: the two hydrophobic interactions of the A and D rings (yellow spheres); the aromatic feature of the quinoline is replaced by the one of the indole (blue ring) and the hydrogen bond donor is preserved (green arrow). In addition to the two hydrogen bond acceptors of the PQ scaffold, two more hydrogen bond acceptors and a negative ionizable area were observed in the new pharmacophore (b). The superposition of the two pharmacophores showed a good overlapping of the common features (Fig. 2 c, d), therefore, based on this similarity we expected activity of the newly designed compounds on $GABA_A$ receptors.

### 2.2. Chemistry

A series of nine compounds (Fig. 3) was synthesized and tested for their activity on α1β3 receptors. In order to explore the activity on these receptors, chemically different substituents were chosen, both for position 5 (-H, -Cl, -OMe) and 4′(-Me, -OMe, -Br).

3-(Aryldiazenyl)-1*H*-2-carboxylic acids **6a-g** were obtained using a four-step synthetic route as outlined in Scheme 1: Ethyl-(2-arylhydrazinylidene)-propanoates **2a-b** were synthesized according to a modified literature procedure starting from the corresponding hydrazine [19]. Treatment of **2b** with polyphosphoric acid at 110 °C gave indolecarboxylates **3b** in moderate yields [19]. Indole carboxylate **3c** was obtained exploiting a published procedure directly from p-methoxyphenylhydrazine [20]. The diazonium salt solutions **4a-c** were prepared by the treatment of a solution of methyl-, methoxy-, or bromo-aniline, respectively, in HCl, with a solution of $NaNO_2$ in ice-cold water. The diazonium salt solutions were immediately used for the azo coupling with carboxylates **3a-c** in the presence of excess potassium carbonate in DMF. The ester precursors were obtained in good yields (65–82%), except for the formation of **5e** (30% yield). Ultimately, hydrolysis of the ester

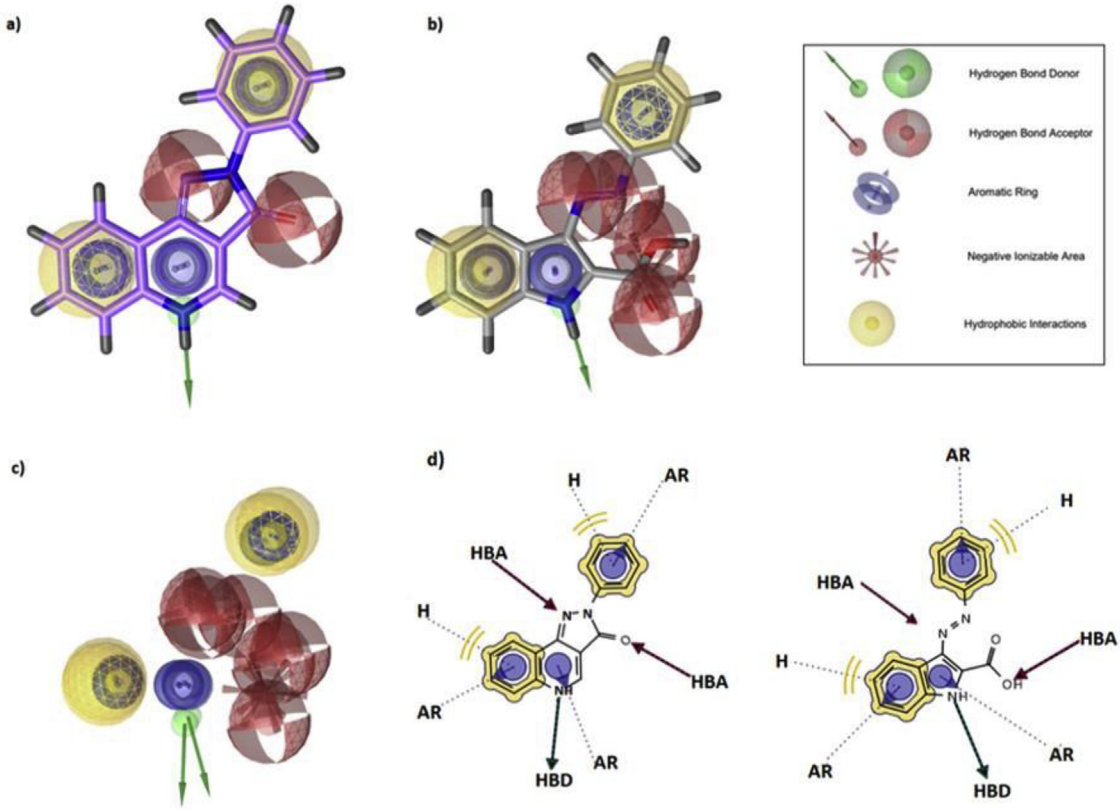


**Fig. 2.** **(a)** The pharmacophore of the PQ scaffold consists of eight features: three aromatic rings (blue ring), two hydrogen bond acceptors (red sphere), one hydrogen bond donor (green arrow) and two hydrophobic features (yellow sphere); **(b)** The pharmacophore of the proposed scaffold has three additional features: two hydrogen bond acceptors (red spheres) and one negative ionizable area (red spikes); **(c)** Superimposition of the pharmacophores of the two scaffolds; **(d)** Schematic representation of the common features of the two scaffolds. (For interpretation of the references to colour in this figure legend, the reader is referred to the Web version of this article.)

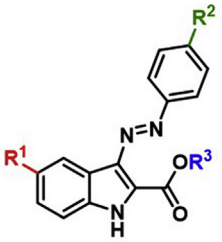


| Compound | $R^1$ | $R^2$ | $R^3$ |
|---|---|---|---|
| 5a | H | OMe | Et |
| 5b | Cl | OMe | Et |
| 6a | H | OMe | H |
| 6b | Cl | OMe | H |
| 6c | OMe | OMe | H |
| 6d | Cl | Br | H |
| 6e | OMe | Br | H |
| 6f | Cl | Me | H |
| 6g | OMe | Me | H |

**Fig. 3.** Overview of tested compounds.

function with a 2 M solution of NaOH gave the final products in 50–70% yield. The structure of the final compound **6b** was supported by X-ray crystallography (Fig. 4). Furthermore, it has to be mentioned that all final compounds **6** showed improved solubility in MeOH and DMSO as compared to their PQ counterparts.

### 2.3. Pharmacological analysis

Two electrode voltage clamp measurements were performed to assess modulatory activity in $\alpha1\beta3$ $GABA_A$ receptors similar as described previously [12]. Fig. 5 provides an overview of the

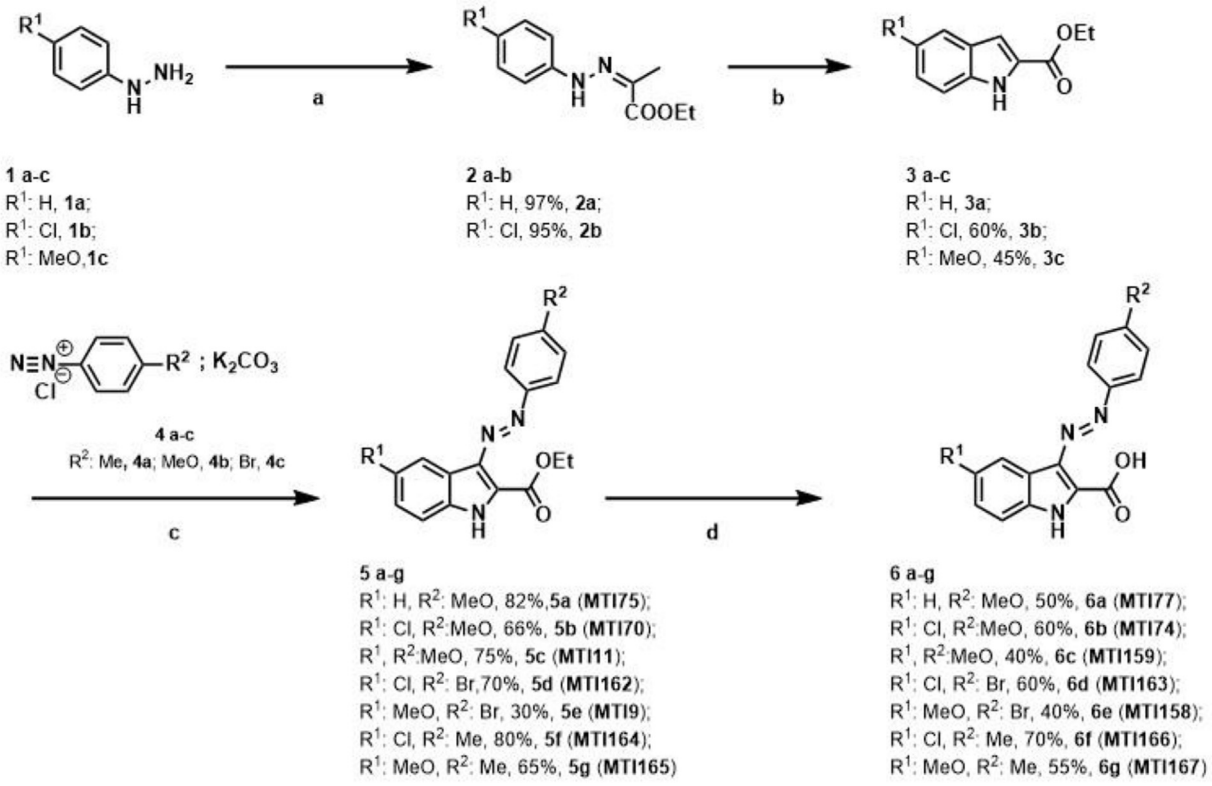


**Scheme 1.** Reagents and conditions: (a) ethylpyruvate, AcOH, EtOH, rf, 2 h; (b) PPA, 110 °C, 5 h for **3b;** ethylpyruvate, $H_2SO_4$, EtOH, 0 °C–45 °C for **3c;** (c) DMF, $K_2CO_3$, 0 °C, 30 min; (d) NaOH (2 N), rf, 3 h.

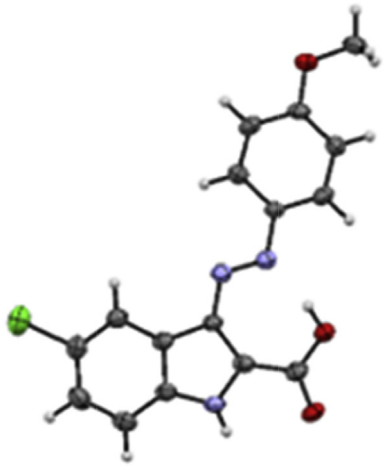

**Fig. 4.** X-ray structure of **6b**.

modulatory effects displayed by the nine compounds at GABA EC3-5 and 30 μM compound concentration which was used to facilitate the comparison with the analogous PQs. Seven (of the total of nine) compounds exhibited modulatory activity in α1β3, with efficacy ranging from moderate to strong. The inactive compounds **5a** and **5b** bear an ester group in position 2 (ring B). Hydrolysis of the ester group on ring B to a carboxylic acid group as in **6a** and **6b** enabled modulation of 200% and 2000% respectively, at 30 μM compound concentration (which is the solubility limit for the analogous PQs) (Fig. 5A). This finding suggests that the carboxylic acid group on ring B is essential for inducing modulation, as indicated by the overlapping of the hydrogen bond acceptor feature of the carboxylic acid of the indole derivatives and the same feature of the carbonyl moiety of the PQs.

Keeping this in mind, different modifications on ring A (position 5) and ring D (position 4′) were introduced in order to test the impact of the substituents on the modulatory efficacy. By analyzing the obtained results some general trends could be identified, which are numerically displayed in panel b of Fig. 5 and graphically summarized in Fig. 6. When looking solely on the different substituents $R^1$, the impact on efficacy follows the rank order chloro *(1800–3000%,* **6f**, **6b** and **6d**) > methoxy (300%–830%, compounds **6e**, **6c** and **6g**) > H *(200%,* **6a**). When analyzing the influence of the $R^2$ residue within a series ($R^1$-Cl or $R^1$-OMe series) it was found that a bromo-substituent in the $R^2$ position results in the highest efficacy in both series (830% **6e** and 3000% **6d**, respectively). The difference between a methoxy or methyl group in $R^2$ is not very pronounced for both series. In the 5-methoxy series, the efficacy with $R^2$ = methoxy (**6c**, 300%) is a bit lower as compared to $R^2$ = methyl (**6g**, 400%). In the 5-chloro series compound **6f** bearing a $R^2$-methyl group, exerted 1800% of the GABA elicited current, whereas up to 2000% were measured with a methoxy group on the same position (**6b**). As expected from the pharmacophore analysis, the new indole-derivatives displayed modulatory properties. To further investigate the similarity of these compounds to the accordingly substituted PQs, we compared their activity with the one of the corresponding published PQs (Fig. 7). As shown in Fig. 7, the modulation of the indole derivatives is comparable or slightly higher in case of the 5-chloroindole derivatives (panel A **6b** vs **7a**, and B **6f** vs. **7b**), and generally significantly lower in the case of the 5-methoxyindole derivatives, compared to the corresponding PQs (panel C **6c** vs. **7c**, and D **6g** vs. **7d**). Assuming that both classes of compound share the α+/β− binding site, this data seem to suggest that the modifications of the PQ scaffold towards the indole

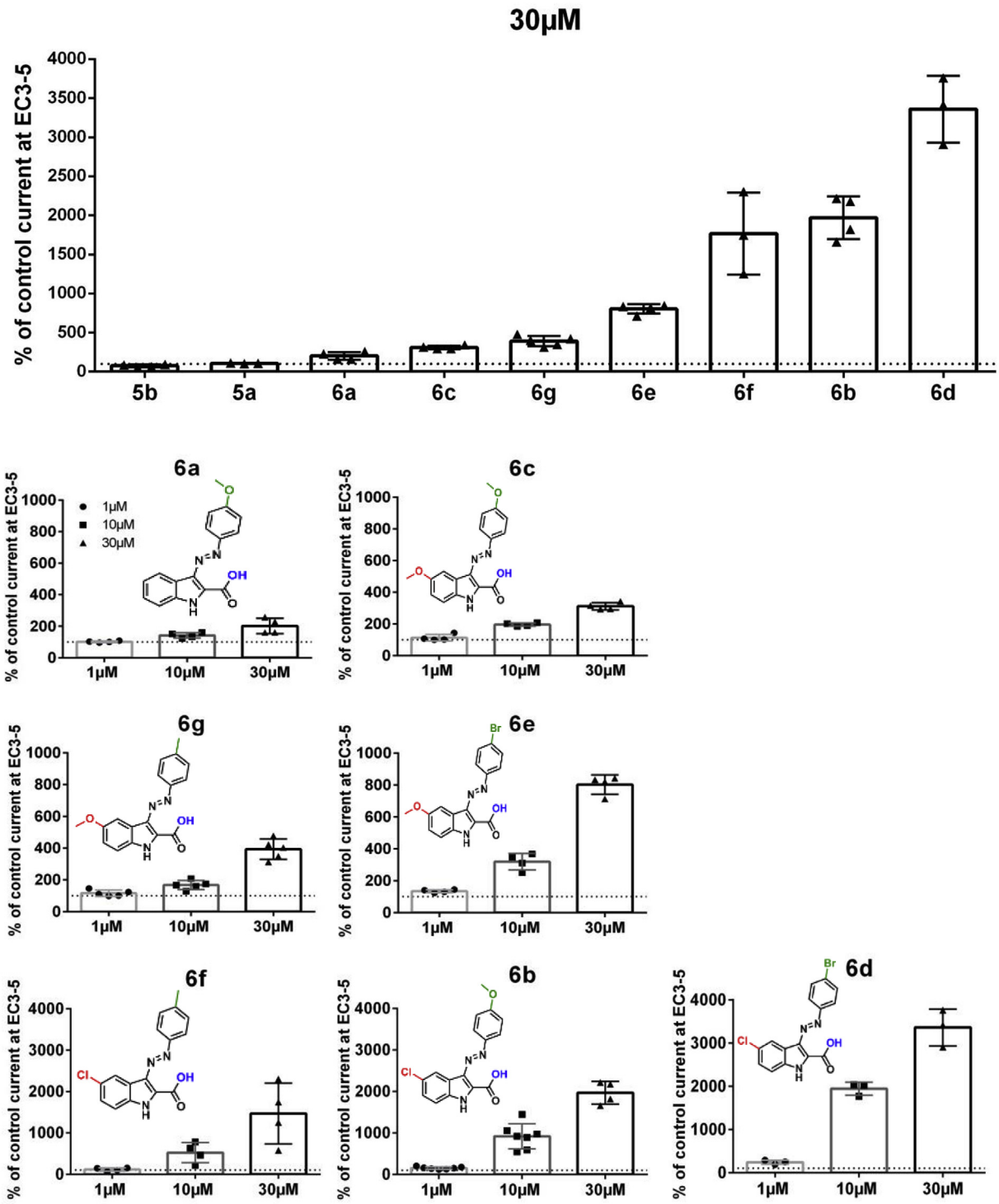


**Fig. 5. Results of the TEV electrophysiological assay.** All compounds were tested in α1β3 subunit injected oocytes using two electrode voltage clamp methods. Panel A displays the modulation of all compounds at 30 μM. Panel B summarizes the modulatory activity of the active compounds at 3 concentrations. Compounds are presented in the order of increasing efficacy. Columns for each concentration represent the mean ± SEM from 3 to 7 oocytes in 2–4 batches. Note the different scales of the y-axes.

derivatives **6**, resulted in a different interaction between the receptor and the R5-substituent on ring A. The corresponding data show that $R^1$ Cl-substituted indole compounds **6b**/**6f** display much higher modulation than the $R^1$-MeO substituted derivatives **6c**/**6g**. This drop of modulation when increasing the size of the substituent on ring A could be attributed to the more flexible geometry of the indole-derivatives which might result in having the methoxy group in an area of the binding site with insufficient space or a repulsive interaction. On the other hand, we do not see a similarly strong effect when comparing the data of compounds **6b** vs. **6f** and **6c** vs. **6g**. Within those pairs of compounds, the $R^1$ substituent is the same, but $R^2$ substituents differ. This indicates that a possible receptor interaction at the position 4′ on ring D has less effect on the modulation ability of the indole derivatives as compared to the

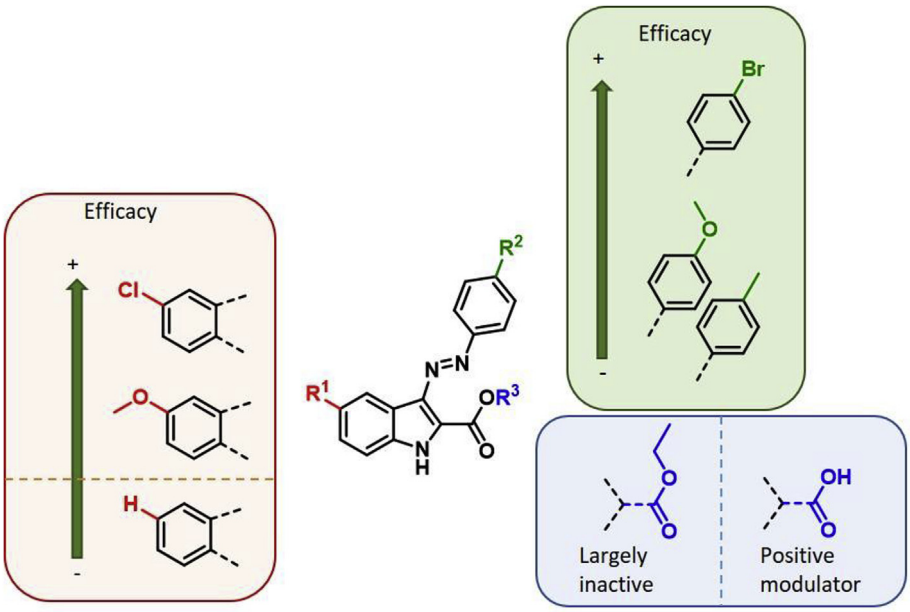


**Fig. 6.** Schematic representation of structure activity relationship.

corresponding PQs. There, **7c** vs. **7d** and especially **7a** vs. **7b** show a recognizable difference in modulation. All these findings are consistent with a closer overlap of ring D in the pocket compared to ring A, which is in line with the pharmacophore model (Fig. 2).

## 3. Conclusions

In this study, we presented a series of 9 indole derivatives **6a-g** with a new scaffold based on the pharmacophore of the PQs. The core structure of the compounds was modified by opening the C-ring, reducing the size of the B-ring and inserting a carboxylic acid moiety. These modifications resulted in a different polarity profile and, hence, better solubility of the compounds. Additionally, different substituents on the rings defined the diverse characteristic of the compounds. The new compounds modulate the recombinant $GABA_A$ receptor combination $\alpha1\beta3$, in *X. laevis* oocytes, whereby a similar SAR also suggests that they share the same binding site with the PQ compounds. We could show that compounds containing a carboxylic acid on ring B and a chlorine atom on ring A exert the highest modulation, whereas indole esters remained inactive. Additionally, the incorporation of a bromine atom on ring D enhanced the efficacy remarkably (Fig. 6). The biological data suggest that the more flexible geometry of the indole derivatives leads to a slightly different spatial exploitation of the binding site. Future modifications of the scaffold will be directed towards proving this hypothesis, and are currently ongoing in our laboratories.

## 4. Experimental

### 4.1. Materials and instrumentation

Organic solvents were purified when necessary by standard methods or purchased from commercial suppliers [21]. Chemicals were purchased from commercial suppliers and used without further purification. TLC was performed using silica gel 60 aluminium plates containing fluorescent indicator from Merck and detected either with UV light at 254 nm or by charring potassium permanganate (1 g $KMnO_4$, 6.6 g $K_2CO_3$, 100 mg NaOH, 100 mL $H_2O$ in 1 M NaOH) with heating. Flash column chromatography (FC) was carried out at Büchi Sepacore™ MPLC system using silica gel 60 M (particle size 40–63 μm, 230–400 mesh ASTM, Macherey Nagel, Düren). Unless otherwise noted all compounds were purified with a ratio of 1/80 (weight (compound)/weight (silica)). All compounds were obtained in a purity greater than 95% according to NMR. NMR spectra were recorded on a Bruker *AC 200* ($^1$H: 200 MHz, $^{13}$C: 50 MHz), Bruker *Avance Ultrashield 400* ($^1$H: 400 MHz, $^{13}$C: 101 MHz) and Bruker *Avance IIIHD 600* spectrometer equipped with a Prodigy BBO cryo probe ($^1$H: 600 MHz, $^{13}$C: 151 MHz). Chemical shifts are given in parts per million (ppm) and were calibrated with internal standards of deuterium labelled solvents $CHCl_3$-*d* ($^1$H 7.26 ppm, $^{13}$C 77.16 ppm) and DMSO-$d_6$ ($^1$H 2.50 ppm, $^{13}$C 39.52 ppm). Multiplicities are denoted by s (singlet), br s (broad singlet), d (doublet), dd (doublet of doublet) and m (multiplet). Melting points were determined with a Büchi Melting Point B-545 apparatus. HR-MS was measured on an Agilent 6230 LC TOFMS mass spectrometer equipped with an Agilent Dual AJS ESI-Source.

### 4.2. Synthesis procedures

**Synthesis of ethyl-(*Z*)-2-(2-phenyl)hydrazinylidene)propanoate 2a** Ethyl pyruvate (1.6 equiv.) and acetic acid (0.2 equiv.) were added to a solution of the hydrazine (1 equiv., 5 g, 0.046 mol) in EtOH (50 mL). The reaction was heated to reflux for 2 h. Upon cooling to room temperature, the product crystalized from the reaction mixture. The crystals were collected by filtration and washed with cold EtOH. **2a:** 9 g, 97%, colourless solid; $^1$H NMR (400 MHz, DMSO-$d_6$) δ 1.26 (t, $J = 7.1$ Hz, 3H), 2.06 (s, 3H), 4.19 (q, $J = 7.1$ Hz, 2H), 6.88 (t, $J = 4.3$ Hz, 1H), 7.27 (d, $J = 4.3$ Hz, 4H), 9.81 (s, 1H); $^{13}$C NMR (101 MHz, DMSO-$d_6$) δ 11.8 (q), 14.3 (q), 60.2 (t), 113.7 (d, 2C), 120.8 (s), 129.0 (d, 2C), 131.7 (s), 144.4 (s), 164.9 (s); M. p. 118–119 °C.

**Synthesis of ethyl-(*Z*)-2-(2-(4-Chlorophenyl)hydrazinylidene)propanoate 2b** Ethyl pyruvate (1.6 equiv.) and acetic acid (0.2 equiv.) were added to a solution of the hydrazine (1 equiv., 4 g, 0.022 mol) in EtOH (30 mL). The reaction was heated to reflux for 2 h. Upon cooling to room temperature, the product crystalized from the reaction mixture. The crystals were collected by filtration

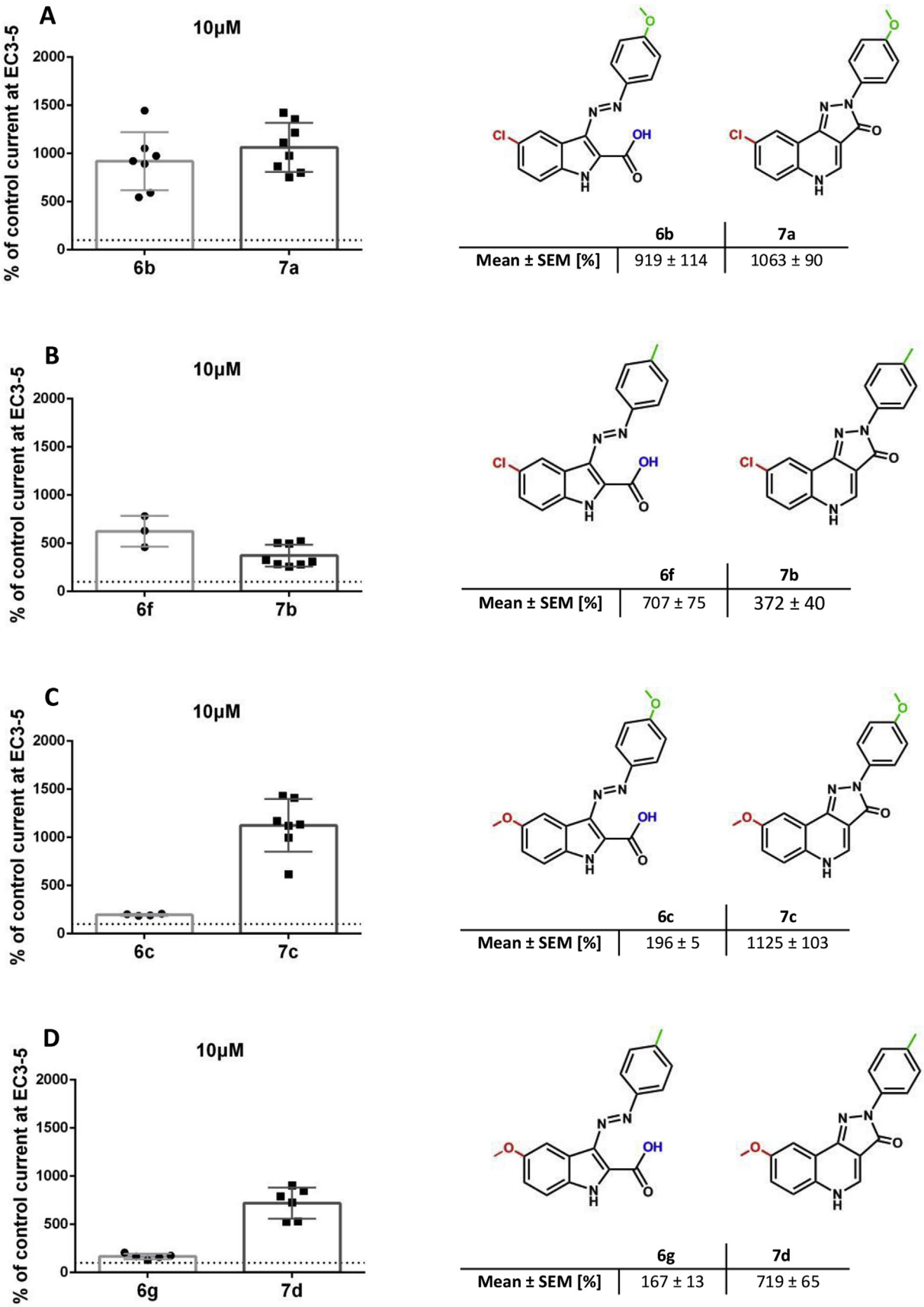


**Fig. 7.** Comparison of indole derivatives with corresponding PQs. The bar graphs show the compounds modulation at 10 µM concentration in α1β3 $GABA_A$ receptors in direct comparison, which are also given numerically below the structures as Mean ± SEM. Values of corresponding PQs are taken from Simeone et al. [6].

and washed with cold EtOH.**2b:** 5.09 g, 95%, yellow crystals; $^1$H NMR (400 MHz, DMSO-$d_6$) δ 1.26 (t, $J$ = 7.1 Hz, 3H), 2.05 (s, 3H), 4.19 (q, $J$ = 7.1 Hz, 2H), 7.19–7.36 (m, 3H), 9.94 (s, 1H); $^{13}$C NMR (101 MHz, DMSO-$d_6$) δ 12.4 (q), 14.7 (q), 60.8 (t), 115.6 (d, 2C), 124.8 (s), 129.4 (d, 2C), 133.2 (s), 143.8 (s), 165.2 (s); M.p. 125–127 °C.

**Synthesis of ethyl 1H-indole-2-carboxylate and ethyl 5-chloro-1*H*-indole-2-carboxylate 3b: 2b** (1 equiv., 6.51 g, 0.027 mol) and polyphosphoric acid (1:10 w/w) were heated at 100 °C for 5 h. The reaction mixture was poured onto ice and the product was extracted with ethyl acetate (3 × 150 mL). The product was purified by silica gel flash column chromatography (crude material:$SiO_2$ = 1:100; ethyl acetate: hexane 1:6 to 1:4) to afford **3b** (5.8 g, 60%) as a colourless solid. $^1$H NMR (400 MHz, DMSO-$d_6$) δ 1.34 (t, $J$ = 7.1 Hz, 3H), 4.34 (q, $J$ = 7.1 Hz, 2H), 7.12 (dd, $J$ = 2.2, 0.9 Hz, 1H), 7.26 (dd, $J$ = 8.8, 2.1 Hz, 1H), 7.46 (dt, $J$ = 8.8, 0.8 Hz, 1H), 7.72 (d, $J$ = 2.1 Hz, 1H), 12.08 (s, 1H);$^{13}$C NMR (101 MHz, DMSO-$d_6$) δ 14.7 (q), 61.1 (t), 107.6 (d), 114.7 (d), 121.5 (d), 125.1 (d), 125.2 (s), 128.2 (s), 129.3 (s), 136.2 (s), 161.5 (s); M. p. 165–166 °C.

**Synthesis of ethyl 5-methoxy-1*H*-indole-2-carboxylate 3c**: 4-Methoxyphenyl-hydrazine (1 equiv., 3 g, 0.017 mol) and ethyl pyruvate (1.1 equiv.) were added consequently to a cooled (0 °C) solution of sulfuric acid (3.7 mL) and ethanol (21 mL). The reaction mixture was stirred for 2 h at room temperature. The temperature was increased to 45 °C and the reaction was stirred overnight. Upon cooling to room temperature, a precipitate formed. The crude mixture was washed with ethyl acetate to afford **3c** as a colourless solid (1.75 g, 46%). $^1$H NMR (400 MHz, $CDCl_3$) δ 1.41 (t, $J$ = 7.1, Hz, 3H), 3.85 (s, 3H), 4.41 (q, $J$ = 7.1, Hz, 2H), 7.00 (dd, $J$ = 8.9, 2.5 Hz, 1H), 7.08 (d, $J$ = 2.4 Hz, 1H), 7.15 (dd, $J$ = 2.2, 1.0 Hz, 1H), 7.31 (dt, $J$ = 9.0, 0.8, 0.8 Hz, 1H), 8.82 (s, 1H); $^{13}$C NMR (101 MHz, $CDCl_3$) δ = 14.6 (q), 55.8 (q), 61.1 (t), 102.7 (d), 108.3 (d), 112.9 (d), 117.1 (d), 128.0 (s), 128.1 (s), 132.2 (s), 154.9 (s), 162.0 (s); M. p. 157–158 °C.

*4.2.1. General procedure for the synthesis of the ester derivatives **5a-g***

Preparation of the diazonium salt solution: The aniline (1equiv.) was dissolved in a solution of HCl 4 M (0.16 w/v) and cooled to 0 °C. Then an ice-cold solution of $NaNO_2$ (0.18 w/v) in water was added dropwise and the reaction was stirred for 10min. The diazonium salt was kept at 0 °C and used immediately after its preparation. Compound **3a**, **3b** or **3c** (1 equiv.) and potassium carbonate (10 equiv.) were suspended in DMF (0.2 M) and cooled to 0 °C. Then a solution of the freshly prepared diazonium salt (1.2 equiv.) was added dropwise. Upon the adding a colourful precipitation formed, the reaction was stirred at 0 °C for 30 min. The reaction was diluted with water and extracted with ethyl acetate. The product was purified by silica gel flash chromatography (crude material:$SiO_2$ = 1:100; ethyl acetate: hexane 1:4).

**Ethyl (*E*)-3-((4-methoxyphenyl)diazenyl)-1*H*-indole-2-carboxylate 5a** The reaction was carried out according to the general procedure for the synthesis of the ester derivatives with 200 mg of **3a** (1 equiv., 1.06 mmol) and delivered **5a** as an orange solid (280 mg, 82%). $^1$H NMR (400 MHz, DMSO-$d_6$) δ 1.43 (t, $J$ = 7.1, 7.1 Hz, 3H), 3.87 (s, 3H), 4.46 (q, $J$ = 7.1, 7.1, 7.1 Hz, 2H), 7.13 (d, $J$ = 8.9 Hz, 2H), 7.28 (dd, $J$ = 8.1, 7.0, 1.0 Hz, 1H), 7.39 (dd, $J$ = 8.2, 6.9, 1.2 Hz, 1H), 7.51–7.56 (m, 1H), 7.92 (d, $J$ = 8.9 Hz, 2H), 8.46 (dd, $J$ = 8.1, 1.0 Hz, 1H), 12.54 (s, 1H); $^{13}$C NMR (101 MHz, DMSO-$d_6$)δ 14.3 (q), 55.6 (q), 61.2 (t), 112.8 (s), 114.5 (d, 2C), 117.4 (s), 123.5 (d, 2C), 123.7 (s), 124.0 (s), 126.1(s), 127.6 (s), 134.7 (s), 135.7 (s), 147.6 (s), 160.8 (s), 161.1 (s); M. p. 220 °C; HR-MS (ESI): 324.1361 $[M+H]^+$; (calcd. 324.1343).

**Ethyl (*E*)-5-chloro-3-((4-methoxyphenyl)diazenyl)-1*H*-indole-2-carboxylate 5b** The reaction was carried out according to the general procedure for the synthesis of the ester derivatives with 80 mg of **3b** (1 equiv., 0.36 mmol) and delivered **5b** as an orange solid (85 mg, 66%). $^1$H NMR (400 MHz, DMSO-$d_6$) δ 1.42 (t, $J$ = 7.1 Hz, 3H), 3.86 (s, 3H), 4.45 (q, $J$ = 7.1 Hz, 2H), 7.12 (d, $J$ = 9.0 Hz, 1H), 7.41 (dd, $J$ = 8.8, 2.2 Hz, 1H), 7.55 (d, $J$ = 8.7 Hz, 1H), 7.92 (d, $J$ = 9.0 Hz, 1H), 8.43 (d, $J$ = 2.1 Hz, 1H), 12.73 (s, 1H); $^{13}$C NMR (101 MHz, DMSO-$d_6$) δ = 14.3 (q), 55.6 (q), 61.4 (t), 114.6 (d, 2C), 114.7 (s), 118.1 (s), 122.7 (d), 123.9 (d, 2C), 126.2 (d), 127.8 (s), 128.7 (s), 133.8 (s), 134.1 (s), 147.4 (s), 160.5 (s), 161.3 (s); M. p. 260–262 °C; HR-MS (ESI): 358.0973 $[M+H]^+$; (calcd. 357.088).

**Ethyl (*E*)-5-methoxy-3-((4-methoxyphenyl)diazenyl)-1*H*-indole-2-carboxylate 5c** The reaction was carried out according to the general procedure for the synthesis of the ester derivatives with 100 mg of **3c** (1 equiv., 0.46 mmol) and delivered **5c** as an orange solid (130 mg, 75%). $^1$H NMR (400 MHz, DMSO-$d_6$) δ 1.43 (t, $J$ = 7.1 Hz, 3H), 3.83 (s, 3H), 3.86 (s, 3H), 4.43 (t, $J$ = 7.1 Hz, 2H), 7.05 (dd, $J$ = 9.0, 2.6 Hz, 1H), 7.12 (d, $J$ = 9.0 Hz, 2H), 7.44 (dd, $J$ = 8.9, 0.5 Hz, 1H), 7.92 (d, $J$ = 9.0 Hz, 1H), 7.95 (d, $J$ = 2.5 Hz, 1H), 12.45 (s, 1H); $^{13}$C NMR (101 MHz, DMSO-$d_6$) δ 14.3 (q), 55.3 (q), 55.5 (q), 61.0 (t), 104.3 (d), 113.9 (s), 114.5 (d, 2C), 116.8 (d), 117.7 (s), 123.6 (d, 2C), 127.6 (s), 130.8 (s), 134.5 (s), 147.5 (s), 156.7 (s), 160.7 (s), 160.9 (s); M. p. 225–226 °C; HR-MS (ESI): 354.1478 $[M+H]^+$; (calcd. 354.1481).

**Ethyl (*E*)-3-((4-bromophenyl)diazenyl)-5-chloro-1*H*-indole-2-carboxylate 5d** The reaction was carried out according to the general procedure for the synthesis of the ester derivatives with 50 mg of **3b** (1 equiv., 0.22 mmol) and delivered **5d** as an orange solid (60 mg, 70%). $^1$H NMR (400 MHz, DMSO-$d_6$) δ 1.42 (t, 1H), 4.46 (q, $J$ = 7.2 Hz, 1H), 7.43 (d, $J$ = 8.8 Hz, 1H), 7.57 (d, $J$ = 8.7 Hz, 1H), 7.78 (d, $J$ = 8.3 Hz, 2H), 7.88 (d, $J$ = 8.3 Hz, 2H), 8.42 (s, 1H), 12.96 (s, 1H); $^{13}$C NMR (101 MHz, DMSO-$d_6$) δ 14.2 (q), 61.5 (t), 114.9 (d), 117.9 (s), 122.6 (d), 123.5 (s), 123.9 (d, 2C), 126.4 (d), 128.4 (s), 132.4 (d, 2C), 133.7 (s), 134.3 (d), 152.1 (s), 160.3 (s); M. p. 228 °C; HR-MS (ESI): 405.99 621 $[M+H]^+$; (calcd. 405.9952).

**Ethyl (*E*)-3-((4-bromophenyl)diazenyl)-5-methoxy-1*H*-indole-2-carboxylate 5e** The reaction was carried out according to the general procedure for the synthesis of the ester derivatives with 180 mg of **3c** (1 equiv., 0.82 mmol) and delivered **5e** as a dark orange solid (100 mg, 30%). $^1$H NMR (400 MHz, DMSO- $d_6$) δ 1.42 (t, $J$ = 7.1, 7.1 Hz, 3H), 3.83 (s, 3H), 4.45 (q, $J$ = 7.1, 7.1, 7.1 Hz, 2H), 7.07 (dd, $J$ = 8.9, 2.6 Hz, 1H), 7.47 (d, $J$ = 8.9 Hz, 1H), 7.78 (d, $J$ = 8.7 Hz, 2H), 7.87 (d, $J$ = 8.7 Hz, 2H), 7.94 (d, $J$ = 2.5 Hz, 1H), 12.69 (s, 1H); $^{13}$C NMR (50 MHz, DMSO) δ = 14.2 (q), 55.3 (q), 61.2 (t), 104.2 (d), 114.1 (d), 117.0 (d), 123.8 (d, 2C), 129.0 (s), 130.8 (s), 132.3 (d, 2C), 152.2 (s), 157.2 (s), 160.4 (s); M. p. 246–248 °C; HR-MS (ESI): 402.0460 $[M+H]^+$; (calcd. 402.0448).

**Ethyl (*E*)-5-chloro-3-(p-tolyldiazenyl)-1*H*-indole-2-carboxylate 5f**: The reaction was carried out according to the general procedure for the synthesis of the ester derivatives with 50 mg of **3b** (1 equiv., 0.22 mmol) and delivered **5f** as an orange solid (55 mg, 80%). $^1$H NMR (400 MHz, DMSO-$d_6$) δ 1.43 (t, $J$ = 7.1 Hz, 3H), 2.41 (s, 3H), 4.47 (q, $J$ = 7.1 Hz, 2H), 7.40 (s, 2H), 7.43 (dd, $J$ = 8.8, 2.2 Hz, 1H), 7.57 (dd, $J$ = 8.8, 0.6 Hz, 1H), 7.85 (d, $J$ = 8.3 Hz, 2H), 8.44 (dd, $J$ = 2.2, 0.6 Hz, 1H), 12.81 (s, 1H); $^{13}$C NMR (101 MHz, DMSO-$d_6$) δ 14.2 (q), 21.0 (q), 61.4 (t), 114.7 (d), 118.0 (s), 122.1 (d, 2C), 122.6 (d), 126.3 (d), 128.0 (s), 129.4 (s), 129.9 (d, 2C), 133.7 (s), 134.1 (s), 140.5 (s), 151.2 (s), 160.4 (s); M. p. 262 °C; HR-MS (ESI): 342.1039 $[M+H]^+$; (calcd. 342.1004).

**Ethyl (*E*)-5-methoxy-3-(p-tolyldiazenyl)-1*H*-indole-2-carboxylate 5g** The reaction was carried out according to the general procedure for the synthesis of the ester derivatives with 50 mg of **3c** (1 equiv., 0.23 mmol) and delivered **5g** as an orange solid (50 mg, 65%). $^1$H NMR (400 MHz, DMSO-$d_6$) δ 1.42 (d, $J$ = 7.1 Hz, 3H), 2.40 (s, 3H), 3.83 (s, 3H), 4.45 (q, $J$ = 7.1 Hz, 2H), 7.05 (dd, $J$ = 8.9, 2.6 Hz, 1H), 7.38 (d, $J$ = 8.1 Hz, 2H), 7.46 (d, $J$ = 8.9 Hz, 1H), 7.81–7.86 (m, 2H), 7.95 (d, $J$ = 2.5 Hz, 1H), 12.54 (s, 1H); $^{13}$C NMR (101 MHz, DMSO-$d_6$) δ = 14.7 (q), 21.5 (q), 55.8 (q), 61.6 (t),

104.7 (d), 114.4 (d), 117.3 (d), 118.1 (s), 122.4 (d, 2C), 128.7 (s), 130.3 (d, 2C), 131.3 (s), 134.9 (s), 140.5 (s), 151.8 (s), 157.3 (s), 161.1 (s); M. p. 226 °C; HR-MS (ESI): 360.1326 $[M+Na]^+$; (calcd. 360.1319).

*4.2.2. General synthesis acid derivatives **6a-g***

The corresponding ester was suspended in a 2 M solution of NaOH (3 mL) and heated to reflux for 3–4h. The reaction was cooled to room temperature acidified with a 2 M solution of HCl and the product was extracted with ethyl acetate. The pure product was obtained after recrystallization in toluene.

**(*E*)-3-((4-methoxyphenyl)diazenyl)-1*H*-indole-2-carboxylic acid 6a. 6a** (80 mg, 50%, red solid) was obtained from **5a** (200 mg, 0.62 mmol). $^1$H NMR (400 MHz, DMSO-$d_6$) δ 3.86 (s, 3H), 7.14 (d, $J$ = 9.0 Hz, 2H), 7.28 (dd, $J$ = 8.1, 7.0, 1.1 Hz, 1H), 7.38 (dd, $J$ = 8.3, 7.0, 1.3 Hz, 1H), 7.47–7.59 (m, 1H), 7.90 (d, $J$ = 9.0 Hz, 2H), 8.43 (dt, $J$ = 8.0, 1.0 Hz, 1H), 12.51 (s, 1H), 13.57 (d, $J$ = 4.3 Hz, 1H); $^{13}$C NMR (101 MHz, DMSO-$d_6$) δ 55.6 (q), 112.9 (d), 114.6 (d, 2C), 118.0 (s), 123.4 (d), 123.6 (d), 123.7 (d, 2C), 125.9 (d), 134.3 (s), 135.5 (s), 147.2 (s), 161.1 (s), 161.9 (s); M. p. >300 °CHR-MS (ESI): 296.1071 $[M+H]^+$; (calcd. 296.1030).

**(*E*)-5-chloro-3-((4-methoxyphenyl)diazenyl)-1*H*-indole-2-carboxylic acid 6b. 6b** (50 mg, 60%, red solid) was obtained from **5b** (90 mg, 0.25 mmol).$^1$H NMR (400 MHz, DMSO-$d_6$) δ 3.87 (s, 3H), 7.14 (d, $J$ = 9.0 Hz, 2H), 7.39 (dd, $J$ = 8.7, 2.2 Hz, 1H), 7.54 (d, $J$ = 8.8 Hz, 1H), 7.91 (d, $J$ = 9.0 Hz, 2H), 8.43 (d, $J$ = 2.1 Hz, 1H), 12.62 (s, 1H); $^{13}$C NMR (151 MHz, DMSO-$d_6$) δ = 55.6 (q), 114.6 (d), 114.6 (d, 2C), 118.7 (s), 122.5 (d), 123.8 (s), 125.8 (d, 2C), 127.6 (s), 133.3 (s), 133.8 (s), 147.3 (s), 161.2 (s), 161.8 (s); M. p. >350 °C; HR-MS (ESI): 330.0664 $[M+H]^+$; (calcd. 330.0640).

**(*E*)-5-methoxy-3-((4-methoxyphenyl)diazenyl)-1*H*-indole-2-carboxylic acid 6c. 6c** (10 mg, 60%, red solid) was obtained from **5c** (20 mg, 0.05 mmol). $^1$H NMR (600 MHz, DMSO-$d_6$) δ 3.83 (d, $J$ = 22.5 Hz, 6H), 6.98 (dd, $J$ = 8.8, 2.6 Hz, 1H), 7.11 (d, $J$ = 8.9 Hz, 1H), 7.42 (d, $J$ = 8.8 Hz, 1H), 7.87 (d, $J$ = 8.9 Hz, 1H), 7.94 (d, $J$ = 2.6 Hz, 1H), 12.19 (s, 1H); $^{13}$C NMR (101 MHz, DMSO-$d_6$) δ 55.7 (q), 56.0 (q), 104.6 (d), 114.2 (d, 2C), 114.9 (s), 116.3 (d), 119.3 (s), 123.9 (d, 2C), 130.7 (s), 133.8 (s), 147.6 (s), 156.9 (s), 161.1 (s), 162.5 (s); M. p. >350 °C; HR-MS (ESI): 326.113 $[M+H]^+$; (calcd. 326.1135).

**(*E*)-3-((4-bromophenyl)diazenyl)-5-chloro-1*H*-indole-2-carboxylic acid 6d. 6d** (30 mg, 60%, red solid) was obtained from **5d** (50 mg, 0.12 mmol). $^1$H NMR (600 MHz, DMSO-$d_6$) δ 7.42 (dd, $J$ = 8.7, 2.2 Hz, 1H), 7.55 (d, $J$ = 8.7 Hz, 1H), 7.78 (d, $J$ = 8.7 Hz, 2H), 7.86 (d, $J$ = 8.6 Hz, 2H), 8.43 (d, $J$ = 2.1 Hz, 1H), 12.86 (s, 1H); $^{13}$C NMR (151 MHz, DMSO-$d_6$) δ 114.8 (d), 118.2 (s), 122.5 (d), 123.4 (s), 123.9 (d, 2C'), 126.1 (d), 128.2 (s), 132.4 (d, 2C), 133.4 (s), 133.9 (s, 2C), 152.0 (s), 161.6 (s); M. p. >300 °C; HR-MS (ESI): 377.9636 $[M+H]^+$; (calcd. 377.969).

**(*E*)-3-((4-bromophenyl)diazenyl)-5-methoxy-1*H*-indole-2-carboxylic acid 6e. 6e** (6 mg, 81%, red solid) was obtained from **5e** (10 mg, 0.06 mmol).$^1$H NMR (400 MHz, DMSO-$d_6$) δ 3.83 (s, 3H), 7.05 (dd, $J$ = 8.9, 2.6 Hz, 1H), 7.45 (d, $J$ = 8.9 Hz, 1H), 7.77 (d, $J$ = 8.7 Hz, 2H), 7.85 (d, $J$ = 8.8 Hz, 2H), 7.93 (d, $J$ = 2.6 Hz, 1H), 12.65 (s, 1H), 13.56 (s, 1H); $^{13}$C NMR (101 MHz, DMSO-$d_6$) δ 55.3 (q), 104.1 (d), 114.0 (d), 116.7 (d), 118.0 (s), 123.0 (s), 123.7 (d, 2C), 129.9 (s), 132.3 (d, 2C), 134.2 (s), 152.0 (s), 157.1 (s), 161.6 (s);M. p. decomposition >260 °C; HR-MS (ESI): 374.0120 $[M+H]^+$; (calcd. 374.0135).

**(*E*)-5-chloro-3-(p-tolyldiazenyl)-1*H*-indole-2-carboxylic acid 6f. 6f** (25 mg, 70%, red solid) was obtained from **5f** (40 mg, 0.11 mmol) and 4 mL of 2 M solution of NaOH. $^1$H NMR (400 MHz, DMSO-$d_6$) δ 2.40 (s, 3H, 7.31–7.44 (m, 3H), 7.55 (d, $J$ = 8.7 Hz, 1H), 7.83 (d, $J$ = 8.3 Hz, 2H), 8.43 (d, $J$ = 2.1 Hz, 1H), 12.75 (s, 1H); $^{13}$C NMR (101 MHz, DMSO-$d_6$) δ 21.0 (q), 114.7 (d), 118.5 (s), 122.0 (d, 2C), 122.5 (d), 126.0 (d), 127.9 (s), 129.9 (d, 2C), 133.4 (s), 133.9 (s, 2C), 140.4 (s), 151.0 (s), 161.6 (s); M. p. decomposition >250 °C; HR-MS (ESI): 314.0696 $[M+H]^+$; (calcd. 314.0691).

**(*E*)-5-methoxy-3-(p-tolyldiazenyl)-1*H*-indole-2-carboxylic acid 6g. 6g** (20 mg, 54%, red solid) was obtained from **5g** (40 mg, 0.12 mmol) and 4 mL of 2 M solution of NaOH·$^1$H NMR (400 MHz, DMSO-$d_6$) δ 2.36 (s, 3H), 3.79 (s, 3H), 7.00 (dd, $J$ = 9.0, 2.5 Hz, 1H), 7.34 (d, $J$ = 7.7 Hz, 2H), 7.40 (d, $J$ = 8.9 Hz, 1H), 7.77 (d, $J$ = 7.9 Hz, 2H), 7.88 (d, $J$ = 2.4 Hz, 1H); $^{13}$C NMR (101 MHz, DMSO-$d_6$) δ = 21.0 (q), 55.3 (q), 103.9 (d), 114.0 (d), 116.6 (s), 118.6 (s), 121.8 (d, 2C), 129.8 (d, 2C), 130.5 (s), 134.1 (s), 140.0 (s), 150.8 (s), 156.8 (s), 161.7 (s); M. p. decomposition >300 °C; HR-MS (ESI): 310.1195 $[M+H]^+$; (calcd. 310.1186).

*4.3. X-ray single crystal diffraction*

Crystals of **6b** (CCDC 1844629) were grown by recrystallization from toluene. X-ray diffraction data were collected in a dry stream of nitrogen on a Bruker Kappa APEX II diffractometer system using graphite-monochromatized Mo-Kα radiation (λ = 0.71 073 Å) and fine sliced φ- and ω-scans. Owing to a reconstructive phase transition below ca. 180 K, the crystal was cooled to T = 200 K. Data were reduced to intensity values with SAINT and an absorption correction was applied with the multi-scan approach implemented in SADABS [22]. The structures were solved by the dual-space approach implemented in SHELXT [23] and refined with JANA2006 [24]. Non-hydrogen atoms were refined anisotropically. The H atoms connected to C atoms were placed in calculated positions and thereafter refined as riding on the parent atoms. The carboxylic acid hydrogen atom was located from difference Fourier maps and refined freely. Contributions of disordered solvents to the intensity data were removed using the SQUEEZE routine of the PLATON software suite [25]. Molecular graphics were generated with the program MERCURY [26].

*4.4. Two-electrode voltage clamp electrophysiology*

All steps were performed as reported previously [6]. In brief, cDNA expression vectors encoding for rat $GABA_A$ receptor subunits α1 and β3 were linearized, transcribed and purified in order to generate mRNA. For the microinjection, the RNA of the α1 and β3 receptor combination was mixed at 1:1 ratio with a final concentration of 56 ng/μl. Mature female *Xenopus laevis* (Nasco, WI) were anaesthetized in a bath of ice-cold 0.17% Tricain (Ethyl-m-aminobenzoate, Sigma, MO) before decapitation and transfer of the frog's ovary to ND96 medium (96 mM NaCl, 2 mM KCl, 1 mM $MgCl_2$, 5 mM HEPES; pH 7.5). Stage 5–6 oocytes with the follicle cell layer around them were roughly dissected with forceps into packages of 10–15 cells and washed in $Ca^{2+}$-free ND96 medium. Cells were then digested with collagenase (type IA, Sigma, NO, 1 mg/ml ND96) at 18 °C shaking at 70 rpm for 20–40 min and gently defolliculated with a pipette. Defolliculated cells were stored at 18 °C for at least 1 h in ND96 solution containing penicillin G (10 000 IU/100 mL) and streptomycin (10 mg/100 mL) in order to preselect and exclude damaged cells from further treatment. Healthy defolliculated oocytes were injected with an aqueous solution of mRNA (2.8ng/oocyte). The injected oocytes were incubated at 18 °C (NDE + penstrep) for 2–3 days for the α1β3 receptors before recording. For electrophysiological recordings, oocytes were impaled with two microelectrodes (1–3 MΩ) filled with 2 M KCl and constantly washed by a flow of 6 mL/min NDE medium [96 mM NaCl, 5 mM HEPES-NaOH (pH 7.5), 2 mM KCl, 1 mM $MgCl_2$ x $6H_2O$, 1.8 mM $CaCl_2x2H_2O$] that could be switched to NDE containing GABA and/or test compounds. Compounds were diluted into NDE from DMSO-solutions resulting in a final concentration of 0.1% DMSO perfusing the oocytes and co-applied with GABA until a peak response was observed. To test for modulation of GABA induced

currents, a concentration of GABA, which was titrated to trigger 3–5% in αβ receptors of the respective maximum GABA-elicited current, was applied to the cell with increasing concentrations of compounds. All recordings were performed at room temperature at a holding potential of −60 mV using a Dagan TEV-200A two-electrode voltage clamp (Dagan Corporation, Mineapolis, MN). Data were digitized, recorded and measured using an Axon Digidata 1550 low-noise data acquisition system (Axon Instruments, Union City, CA). Data acquisition was done using pCLAMP v.10.5 (Molecular Devices™, Sunnyvale, CA). Data were analysed using GraphPad Prism v.6. and plotted as bar diagrams/bar graphs. Data are given as mean ± SEM from at least three oocytes of two and more oocyte batches.

## Acknowledgements

This work was financially supported by Austrian Science Fund FWF grant W1232 (graduate school program MolTag). The academic license for LigandScout 4.2.1 was kindly provided by Inte:-Ligand GmbH.

## Appendix A. Supplementary data

Supplementary data to this article can be found online at https://doi.org/10.1016/j.ejmech.2019.07.008.

## References

[1] S. Masiulis, R. Desai, T. Uchański, I. Serna Martin, D. Laverty, D. Karia, T. Malinauskas, J. Zivanov, E. Pardon, A. Kotecha, J. Steyaert, K.W. Miller, A.R. Aricescu, Nature 565 (2019) 454–459.
[2] N. Yokoyama, B. Ritter, A.D. Neubert, J. Med. Chem. 25 (1982) 337–339.
[3] N.J. Katzman, H.E. Shannon, J. Pharmacol. Exp. Ther. 235 (1985) 589–595.
[4] R.W. Olsen, W. Sieghart, Neuropharmacology 56 (2009) 141–148.
[5] W. Sieghart, J. Ramerstorfer, I. Sarto-Jackson, Z. Varagic, M. Ernst, Br. J. Pharmacol. 166 (2012) 476–485.
[6] X. Simeone, D.C.B. Siebert, K. Bampali, Z. Varagic, M. Treven, S. Rehman, J. Pyszkowski, R. Holzinger, F. Steudle, P. Scholze, M.D. Mihovilovic, M. Schnürch, M. Ernst, Sci. Rep. 7 (2017) 5674–5685.
[7] M. Treven, D.C.B. Siebert, R. Holzinger, K. Bampali, J. Fabjan, Z. Varagic, L. Wimmer, F. Steudle, P. Scholze, M. Schnürch, M.D. Mihovilovic, M. Ernst, Br. J. Pharmacol. 175 (2018) 419–428.
[8] W. Sieghart, M.M. Savić, Pharmacol. Rev. 70 (2018) 836–878.
[9] R. Puthenkalam, M. Hieckel, X. Simeone, C. Suwattanasophon, R.V. Feldbauer, G.F. Ecker, M. Ernst, Front. Mol. Neurosci. 9 (2016).
[10] U. Rudolph, H. Möhler, Curr. Opin. Pharmacol. 6 (2006) 18–23.
[11] S.A. Forman, K.W. Miller, Anesth. Analg. 123 (2016) 1263–1273.
[12] Z. Varagic, L. Wimmer, M. Schnürch, M.D. Mihovilovic, S. Huang, S. Rallapalli, J.M. Cook, P. Mirheydari, G.F. Ecker, W. Sieghart, M. Ernst, Br. J. Pharmacol. 169 (2013) 371–383.
[13] M. Mortensen, T.G. Smart, J. Physiol. 577 (2006) 841–856.
[14] J. Ramerstorfer, R. Furtmüller, I. Sarto-Jackson, Z. Varagic, W. Sieghart, M. Ernst, J. Neurosci. 31 (2011) 870–877.
[15] J. Nilsson, R. Gidlöf, E.Ø. Nielsen, T. Liljefors, M. Nielsen, O. Sterner, Bioorg. Med. Chem. 19 (2011) 111–121.
[16] D.E. Knutson, R. Kodali, B. Divović, M. Treven, M.R. Stephen, N.M. Zahn, V. Dobričić, A.T. Huber, M.A. Meirelles, R.S. Verma, L. Wimmer, C. Witzigmann, L.A. Arnold, L.-C. Chiou, M. Ernst, M.D. Mihovilovic, M.M. Savić, W. Sieghart, J.M. Cook, J. Med. Chem. 61 (2018) 2422–2446.
[17] G. Wolber, T. Langer, J. Chem. Inf. Model. 45 (2005) 160–169.
[18] O.F. Güner, J.P. Bowen, J. Chem. Inf. Model. 54 (2014) 1269–1283.
[19] F. Zhang, Y. Zhao, L. Sun, L. Ding, Y. Gu, P. Gong, Eur. J. Med. Chem. 46 (2011) 3149–3157.
[20] T.O. Schrader, B.R. Johnson, L. Lopez, M. Kasem, T. Gharbaoui, D. Sengupta, D. Buzard, C. Basmadjian, R.M. Jones, Org. Lett. 14 (2012) 6306–6309.
[21] W.L.F.C. Armarego, C.L. L, Purification of Laboratory Chemicals, seventh ed., 2012.
[22] Bruker Computer Programs: APEX2, SAINT and SADABS, Bruker AXS Inc., Madison, WI, 2015.
[23] C.F. Macrae, P.R. Edgington, P. McCabe, E. Pidcock, G.P. Shields, R. Taylor, M. Towler, J. van de Streek, J. Appl. Crystallogr. 39 (2006) 453–457.
[24] V. Petrícek, M. Dušek, L. Palatinus, Z. für Kristallogr. - Cryst. Mater. 229 (2014) 345–352.
[25] G. Sheldrick, Acta Crystallogr. A 71 (2015) 3–8.
[26] A. Spek, Acta Crystallogr. D 65 (2009) 148–155.